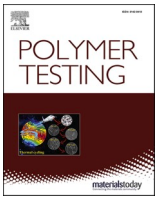
Polymer Testing 131 (2024) 108330



Contents lists available at ScienceDirect

Polymer Testing

journal homepage: www.elsevier.com/locate/polytest





XLPE high voltage insulation; A link between DC conductivity and microstructure

Amir Masoud Pourrahimi [a,*], Claire Pitois [a], Amirhossein Abbasi [b]

[a] NKT HV Cables AB, Technology Consulting, SE-722 26, Västerås, Sweden
[b] NKT HV Cables AB, R&D, SE-371 23, Karlskrona, Sweden

ARTICLE INFO

Keywords:
XLPE
Microstructure
Relaxation processes
DC conductivity
HVDC

ABSTRACT

Crosslinked low-density polyethylene (XLPE) with its simple chemical composition is currently used as the most promising material for the insulation layer in extruded power cables. The processability of low-density polyethylene during extrusion followed by its crosslinking results in an infusible network that withstands high operating temperatures. One of the most important electrical properties that determine the insulation performance is the high voltage DC conductivity (direct-current conductivity under a high electric field). A lower DC conductivity at elevated temperatures decreases the losses in the insulation and hence lowers the risk of thermal runaway. The DC conductivity in pure polyethylene (PE) is predominantly due to electronic transport, and in the case of XLPE the DC conductivity is also affected by the combined effects of the concentration of crosslinking byproducts and the semicrystalline microstructure. The semicrystalline microstructure is complex, and it includes the lamellar morphology, the micrometer-sized superstructure, and the degree of crystallinity. These parameters inter-play to affect the final DC conductivity. This article first describes an overview of XLPE insulation of extruded HVDC cable and then addresses the less-known link among polymer processing, microstructure, and macroscale property (DC conductivity) of XLPE. The revealing of this link leads to a deep understanding of XLPE microstructure and possible ways to improve XLPE insulating properties during polymer processing.

1. Introduction

Polyethylene (PE) is the simplest hydrocarbon polymer, which is produced by the polymerization of ethylene monomer; see Fig. 1. The applications of PE products could vary from low-tech (e.g. garbage bags) to high-tech such as implants, high-strength fibers, and high-voltage (HV) insulations. How is it possible to get this wide range of applications from a simple chemical structure of ethylene monomer? The polymerization process controls the molar mass distribution, and the type and degree of chain branching (long and short chain branching known as LCB and SCB, respectively). These parameters determine different grades of PE; low-density PE (LDPE), high-density PE (HDPE), and linear low-density PE (LLDPE) [1–3]. The SCB affects the crystallization of the polymer chains and consequently, the semi-crystalline microstructure, while the LCB alters the free volume, molecular relaxation processes, and consequently the processability [4–6]. The microstructure is also affected by polymer processing conditions (extrusion, compounding, blow, compression, and injection molding) and post-processing conditions (cooling profile, annealing …). Microstructure here refers to the crystallinity, the crystal thickness, and the spherulitic superstructure of semicrystalline PE. PE has stacks of ca. 10 nm crystal lamellae sandwiched with intermediate amorphous layers shaped into micrometer-sized supramolecular spherulites [4]. The microstructure determines the macro-scale properties (thermal, mechanical, and electrical), and based on these properties, different PE products with a varying range of applications are achievable [2]. The journey from the molecular level to macro-scale properties is sometimes referred to as a “bottom-up” strategy. In all applications, it is demanding to get higher performance in the relevant macro-scale property with a lower risk of diminishing other properties. Therefore, another journey is required in the opposite direction, a so-called “top-down” strategy, to understand deeply the behavior of the current material in the final application. Based on the learning from the top-down strategy, the material could be optimized in the next round of the bottom-up strategy, and therefore a better material that meets the newer requirements could be achieved.

* Corresponding author.
E-mail address: Amir.Pourrahimi@nkt.com (A.M. Pourrahimi).

https://doi.org/10.1016/j.polymertesting.2024.108330
Received 29 November 2023; Received in revised form 28 December 2023; Accepted 4 January 2024
Available online 5 January 2024
0142-9418/© 2024 The Authors. Published by Elsevier Ltd. This is an open access article under the CC BY-NC-ND license (http://creativecommons.org/licenses/by-nc-nd/4.0/).

1.1. XLPE in the power cable industry

One of the "applications" of the PE is the extruded power cables, as shown in Fig. 1. The key component of extruded power cables is the insulation layer. Crosslinked low-density polyethylene (XLPE) is an established material being used as the insulation layer of extruded power cables with continuing high performance. Here, the DC conductivity of insulation is considered the main macro-scale property that defines the performance of power cable resulting in a low-transmission loss for long distances. This makes the transmission of electric power, from renewable sources in distant regions (solar, hydro, and wind) to urban areas, more robust. XLPE has one of lowest DC conductivity among different polymers, which depending on grade and type, is in the range of 10^{-2}–10^{3} fS/m for electric fields of 10–50 kV/mm and temperatures varying from 20 °C to 90 °C [7–10]. The XLPE was developed by General Electric Company in 1963, and it was used as insulation in medium-voltage (MV) cables in 1968. By 1991 more than 90 % of all cables installed in Japan were based on XLPE insulation. The first HVDC extruded XLPE cables were stepped into the market by ABB in 1998 with a transmission voltage of 80 kV, which led to the installation of the first extruded high-voltage direct-current (HVDC) cable in Gotland, Sweden [11]. In 2017, NKT made another milestone and launched the first 640 kV extruded DC underground capable of 3 GW power transmission [12–14].

Besides XLPE's low DC conductivity, it has other desired properties due to its molecular structure and semi-crystalline microstructure. The base LDPE (before crosslinking) has a moderate molecular weight (e.g. Mn ≈ 21 kg mol^{-1}, PDI ≈ 6) [15] and is highly branched with both LCBs (at least 1–2 per 1000 carbons) and SCBs (10–50 per 1000 carbons) [16]. It should be noted the provided data are here based on the typical LDPEs that can be used in the insulation layer of power cables. This high branching level results in high shear thinning and a low melt viscosity during extrusion, leading to good processability in the case of extruded power cables [16]. This molar mass distribution and branching level results in a semicrystalline structure with mass crystallinity of ca. 40 %, melting peak of ca. 110 °C, and crystal and amorphous thicknesses of ca. 9 and ca. 14 nm, respectively [17]. This semicrystalline microstructure results in good mechanical properties; low enough stiffness and high enough fracture toughness for power cable insulation at low temperatures, while it could be bent on cable drums for storage and transport. The presence of crosslinks in XLPE is required to withstand elevated operating temperatures in power cables. The most common way of crosslinking XLPE is through radical crosslinking of LDPE initiated by the thermal decomposition of a peroxide crosslinking agent such as dicumyl peroxide (DCP) into radicals. By abstraction of hydrogen from the LDPE polymer chain, macroradicals are generated as free-radical initiator sites. The combination of free-radical macromolecules quickly leads to the formation of crosslinks, leaving the byproducts of cumyl alcohol, acetophenone, water, and methane, which should be degassed [18]. The gel content of XLPE is high, ~70 % indicative of high crosslinking density (6 per 1000 carbons), which results in a small elongation in the hot-set test and consequently in a high creep-resistant material at elevated temperature above the LDPE melting point [18–20]. The creep-resistant behavior in XLPE due to crosslinks can increase the limiting temperature in short circuit faults up to 250 °C, wherein this temperature could be much lower in thermoplastics. Besides these desired thermomechanical properties, the thermal conductivity of XLPE is high enough to dissipate the heat faster, which allows the cable insulation thicker as compared to suggested thermoplastic insulation e.g. PP [21]. The combination of these properties cannot be easily found for another commodity polymer candidate.

The "bottom-up" and "top-down" strategies are also applicable in the development of XLPE insulations in extruded power cables. Starting with the bottom-up strategy and the molecular level, the polymer supplier industries have been substantially reducing the impurity level in raw materials (for example keeping the content of catalyst in the high-pressure polymerization of LDPE at ultralow levels), while the performance of macro-scale properties such as low DC conductivity, high dielectric strength, high fracture toughness, high creep-resistance at elevated temperature, etc. should be kept high. Besides, the impurity level from external sources is monitored by a cable checker in a systematic sampling manner. The cable checker detects defects in the insulation layer; e.g. cavities, contaminants, and electrical/water trees. For this analysis, the outer Semicon layer is removed, and the cable sample is inserted into the hot oil bath, where the crystalline part of XLPE insulation melts and the sample becomes transparent. With the aid of a light source combined with a high-resolution microscope, the defects could be revealed. The cleanness of filters on the extrusion crosshead are also continuously checked in cable manufacturing.

The formulation of LDPE with crosslinking agents is usually sent from the supplier to the cable manufacturer. The cable manufacturer could also soak/dry the LDPE pellets with crosslinking agents. In cable production, the pellets first are molten during extrusion, providing high enough melt flow (i.e. low enough melt viscosity). The extrusion temperature should be low enough to avoid the decomposition of DCP, but at the same time higher than the melting temperature of LDPE, ca. 110 °C. The cable insulation is usually cured in a Continuous-Vulcanizing (CV) tube at a temperature of 250–390 °C and pressure of

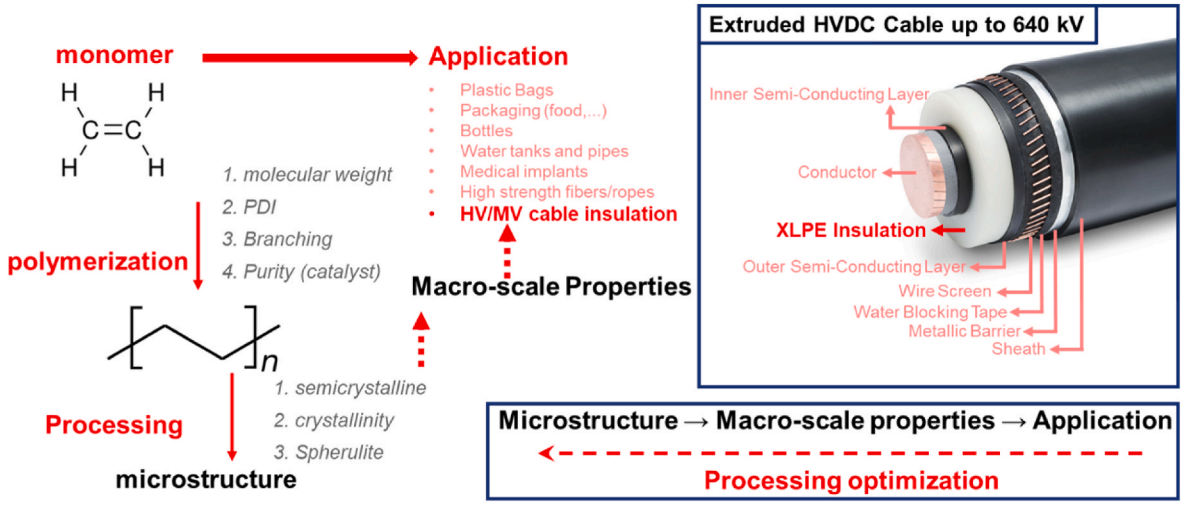


Fig. 1. PE from monomer to the application; Looking from a broader perspective highlighting the "bottom-up" and "top-down" strategies. The use of PE in the "Application" of extruded cable as the insulation layer is highlighted.

7–14 bars [22]. During crosslinking, the viscosity and elasticity increase very rapidly even with minor conversions of DCP, wherein the flowable LDPE melt is replaced with XLPE with high rubbery elasticity. There are other crosslinking technologies in cable industries, such as silane crosslinking and electron-beam crosslinking, which are not discussed here.

For the post-curing process, one should think of how the molten meanwhile rubbery-elastic XLPE cable is cooled. In the cooling process, the XLPE is crystallized mainly in an inert nitrogen atmosphere. The cooling rate controls the microstructure, which in turn determines the electrical and thermomechanical performances. The crystallization process of XLPE on small sizes could be fast, however, the large thickness of insulation and the temperature gradient across the insulation thickness affect the crystallization process. The cooling phase is not only about the temperature and cooling rate. The extensional and shear forces during the cooling phase after the curing create residual mechanical stresses leading to problems such as shrinkback, and further poor electrical performance and detachment insulation from the conductor [22].

As stated earlier, the crosslinking by use of DCP results in unwanted byproducts, which should be removed in a post-extrusion heat-treatment process, named “degassing”. The high concentration of mobile polar byproducts results in the accumulation of charge carriers, and an increase in DC conductivity, while a very low concentration of byproducts could act as trapping sites for charge carriers and reduce the DC conductivity [23–26]. The post-heat treatment temperature increases the diffusion coefficient of mobile species and makes the degassing process faster. This post-heat treatment process also may lead to changes in the semicrystalline microstructure [9,25].

By top-down characterization, it is possible to determine the macro-scale properties (e.g., DC conductivity, stiffness, processability, thermal conductivity, etc.) and correlate them to residual stresses, microstructure, and impurity level. This correlation is very important and helps to increase the performance by improving the characteristics of the raw material (e.g., molecular weight, PDI, branching, comonomer type and content, and catalyst level in case of LDPE), using new additives (e.g., crosslinking coagent, scorch retardant, voltage stabilizer), curing, cooling and degassing processes (e.g., temperature, pressure, time).

In this paper, the correlation between the macro-scale property and the microstructure in XLPE is addressed. The most important and representative macro-scale property in the case of HVDC insulation is DC conductivity. The microstructure here is related to the semicrystalline structure and morphology of XLPE from the nanoscale to the micro-scale. The relaxations are related to molecular motions above the glass transition temperature (T_g). It should be noted that the relaxation in the molecular level and microstructure parameters are inter-acting to determine the final macro-scale property. However, this paper attempts to show their independent impacts on DC conductivity.

2. Macro-scale property; DC conductivity

As stated earlier, the DC conductivity of XLPE is the key macro-scale property that defines its performance in HVDC extruded cable. In this section, the DC conductivity of XLPE samples in plaque shape is discussed with two specific samples that are prepared with different protection films during hot-pressing. For plaque or plate samples, the XLPE was hot-pressed with different protection layers of aluminum (Al) or polyethylene terephthalate (PET, known by the trade name of Mylar) [9]. To show the differences between these two samples, the light optical microscope (LOM) was used to assess the surfaces of XLPE. Fig. 2 shows the images taken from the protection films and their corresponding XLPE surfaces, which were in contact with the protection films. The Mylar has cyclic oligomers on its surfaces that migrate to the XLPE surfaces during compression molding (hot-press). The leakage current (here shown as apparent DC conductivity) was measured under an electric field of 30 kV/mm with thermal cycling between 20 and 70 °C using a three-electrode HV setup, Fig. 3. During the isotherm of 70 °C, the DC conductivity decreased rapidly and reached a slower-changing or quasi-steady state. The Mylar-pressed XLPE plaque samples have higher DC conductivities than the Al-pressed sample. The higher DC conductivities were also detected for LDPE samples that were pressed with Mylar [10,27]. This increase in DC conductivity for Mylar pressed

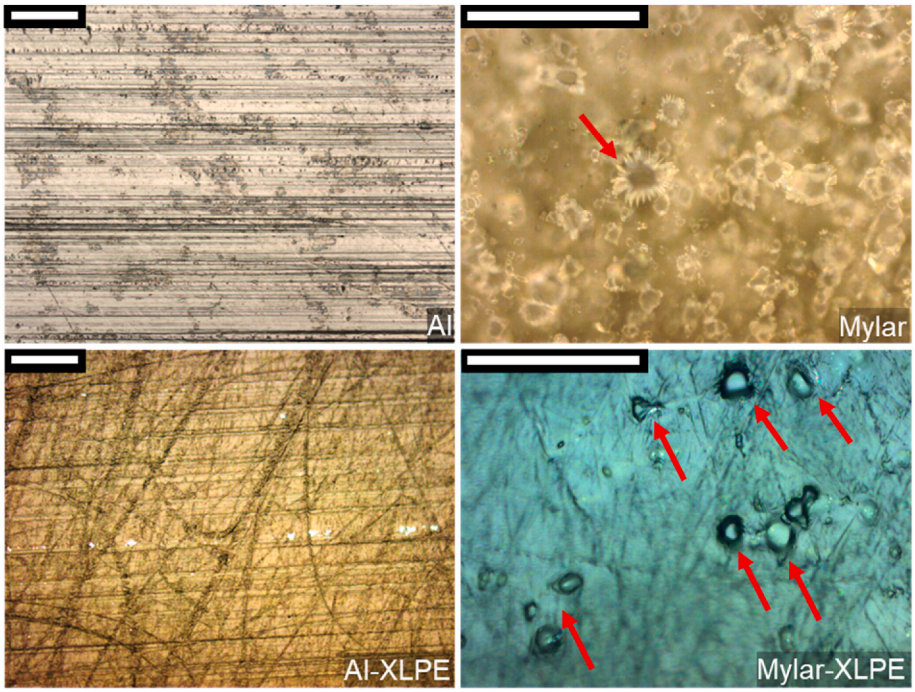


Fig. 2. The LOM images from the surfaces of protection films and their corresponding hot-pressed XLPE plaque samples. The presence of cyclic oligomers is shown by red arrows. The scale bars are 100 μm [9]. Copyright 2022, with permission from IEEE. (For interpretation of the references to colour in this figure legend, the reader is referred to the Web version of this article.)

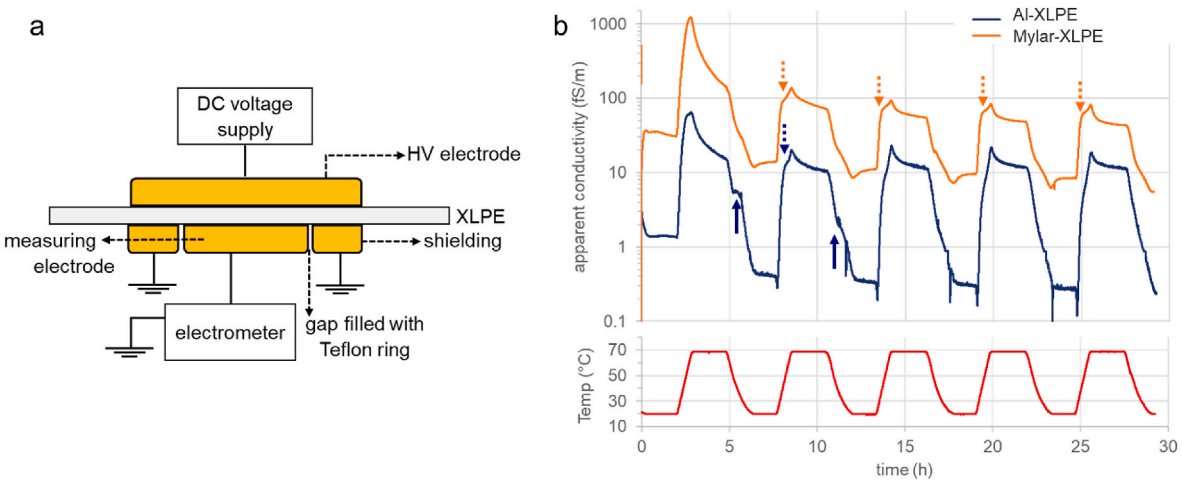


Fig. 3. a) The three-electrode measurement setup for HV DC conductivity, b) apparent HV DC conductivities of XLPE plaque samples with a thickness of 1 mm hot-pressed with Al and Mylar protection films, wherein the appearance of heating and cooling peaks are shown by dashed and solid arrows, respectively [9]. Copyright 2022, with permission from IEEE.

sample could be related to the migration of cyclic oligomers from Mylar to XLPE or LDPE during the compression molding process (i.e. hot-press) [9]. Degassing of these XLPE results in the reduction of DC conductivity by more than one order of magnitude [10,28]. Therefore, it suggests that the presence of cyclic oligomers (stemming from Mylar protection film) on the XLPE surface and or crosslinking byproducts in the bulk of XLPE increases the DC conductivity.

During heating and cooling, peaks/knees were detected as shown by arrows in Fig. 3b. The appearance of the peaks could be shown with non-monotonic Arrhenius temperature dependence of DC conductivity during heating and cooling. According to the conduction mechanism, the DC conductivity is dependent on temperature by an Arrhenius equation with specific activation energy. The appearance of DC conductivity peaks results in non-monotonic Arrhenius temperature dependence meaning that in the semi-logarithmic plot of apparent DC conductivity versus reciprocal temperature, the dependence deviates from a perfect line with a negative slope [27]. Ghorbani et al. [10,27,28] studied the XLPE and LDPE plaque samples using different protection films of Al and Mylar and observed a stronger deviation from Arrhenius temperature dependence during cooling mainly for LDPE and XLPE pressed with Mylar. In another study with the aid of a pulsed electroacoustic (PEA) system, it was shown that the cooling conductivity peak could be correlated to the hetero-charge formation in the case of Mylar-pressed XLPE plaque samples [29]. For XLPE pressed with Mylar, the conductivity peak disappeared after degassing of byproducts. Since the LDPE pressed with Mylar also showed the non-monotonic Arrhenius temperature dependence, the appearance of the peak could not be related to crosslinking byproducts since LDPE is not crosslinked. The appearance of this peak could therefore have originated from two sources (either separate or combined impact):

1. Chemical impurity/contamination introduced from protection films (especially Mylar). This already increases the hetero-charge formation and DC conductivity level.
2. Physical process or thermal history during the hot-press, cooling, and degassing. This could be explained by microstructure.

The 1st reason is already discussed in another study and would not be the scope of this article [10,27,28]. The 2nd reason or source for the appearance of the peak will be discussed later in "The link between microstructure and DC conductivity" Section.

3. Microstructure

In this section, the microstructure of PE (mainly LDPE and XLPE) is introduced. During the cooling from the molten state, PE (e.g. LDPE and XLPE) forms a spherulitic superstructure on the microscale as revealed by the optical microscope. By looking into spherulites in the nanoscale, the sandwich layers of crystal lamella with intermediate amorphous layers can be detected using scanning or transmission electron microscopy (SEM or TEM). The use of these techniques could be complex and needs specific sample preparation, meanwhile, they are reliable locally in the micro- and nanoscale and could not be representative for the bulk of the sample. The thermal analysis with the aid of differential scanning calorimetry (DSC) allows an easier sample preparation and is more representative of the sample bulk (however still on the milligrams level), which will be thoroughly discussed here.

Fig. 4 shows the effect of crosslinking from the molecular level and its impact on the molecular chain and formation of the superstructure on the microscale. The formation of crosslinks (chemical networks) was mentioned earlier. It should be noted that the entanglements or physical network present in LDPE can contribute to crosslinking density [18,30]. During the cooling from the molten state, the crosslinks lead to a different crystallization rate, spherulite morphology/size, crystallinity, crystal lamella thicknesses, and inter-lamella amorphous phase of XLPE compared to pure LDPE [18,25,31]. The crystalline regions (i.e. the crystal lamellae) do not contain crosslinks, and therefore the crosslinks are considered defects; see Fig. 4b. The crosslinks hinder the mobility of the chains, which is expected to hinder the molecular motion and reorganization of semicrystalline structure as shown in Fig. 4b and c (it will be discussed later). The higher amount of DCP or higher crosslinking degree reduces the degree of crystallinity, spherulitic size/shape, and crystal thickness [31]. For example, by the addition of higher content of DCP into the LDPE and increasing the degree of crosslinking, the spherical shape of spherulites changed to axialites with reducing sizes from ca. 15 to 3 μm [31], Fig. 4d. All these changes in microstructure could impact the final macro-scale properties (thermomechanical and thermoelectrical).

Occasionally, the concepts of semicrystalline microstructure, spherulite size, crystallinity, and crystal thickness could be misused or misplaced. These are different concepts, and they do not follow each other necessarily. During the crystallization of XLPE, the micrometer-sized spherulites are formed. The spherulites are built from stacks of nanometer-sized crystal lamellae sandwiched with intermediate amorphous layers, wherein the crystal thicknesses are in the range of 2–12 nm. The crystallinity is related to the partial population of crystals. All

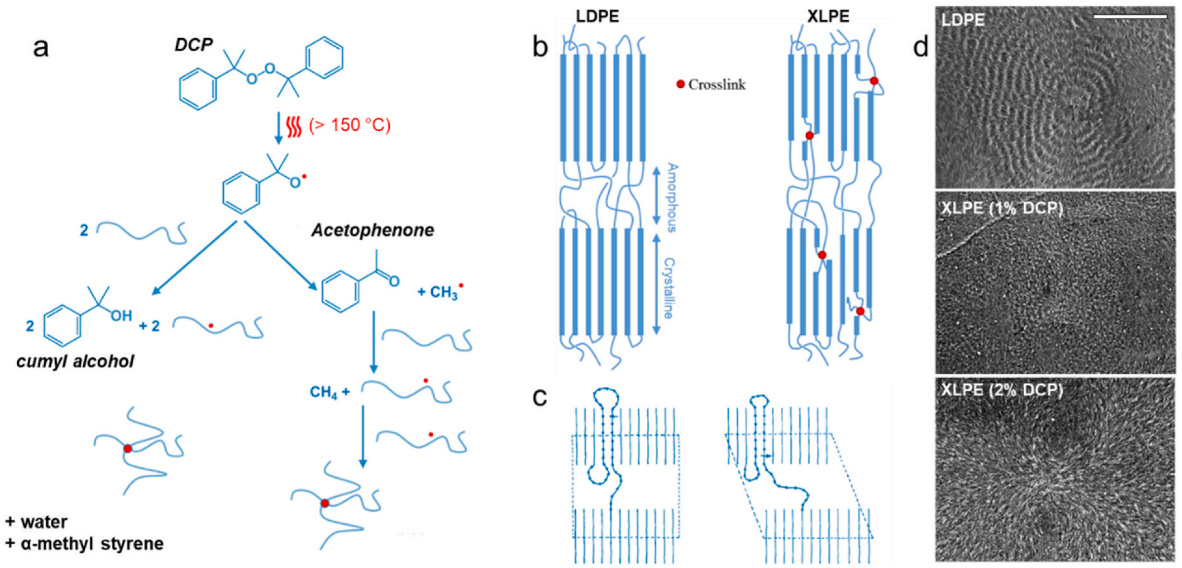


Fig. 4. Formation of XLPE via crosslinking of LDPE and its impact on the semicrystalline microstructure; a) radical crosslinking of LDPE with DCP [18], b) sandwich structure of crystal lamellae and amorphous layers [18] c) molecular relaxation of mechanical α process and its impact on the reorganization of interface crystal and amorphous layers [32], d) spherulitic structures (the scale bar is 5 μm) [31]. a and b) Reproduced with permission [18]. Copyright 2019, M. Mauri, c) Reproduced with permission [32] Copyright 1985, Elsevier, d) Reproduced with permission [31] Copyright 2010, Elsevier.

these parameters could be either directly or indirectly characterized and obtained based on simple methods using DSC instruments. The method should include the first heating, intermediate cooling, and second heating in the temperature range that at least covers the range between glass transition and melting point, i.e., $T_g - T_m$. PE shows three relaxation processes namely γ, β, and α; wherein the β process is associated with the glass-rubber relation known as T_g [32]. The desirable temperature range is suggested to be -50 – 150 °C for PE samples. In the first heating thermogram, the sample shows its thermal history from processes such as extrusion, compounding, hot-press, degassing, and annealing. In the second heating thermogram, the thermal history is already erased from the sample, and it is used to obtain the crystallinity, melting point, and crystal thickness distribution without the impact of thermal history. The crystallization behavior could be studied in the intermediate cooling thermogram.

Fig. 5 shows the use of DSC thermograms of LDPE and XLPE samples to obtain different semicrystalline microstructure parameters such as crystal thickness, crystallization temperature, and degree of crystallinity. PE shows the main melting point at ca. 110 °C with a broad shoulder that continues to ca. −50 °C, Fig. 5a. This board area could be

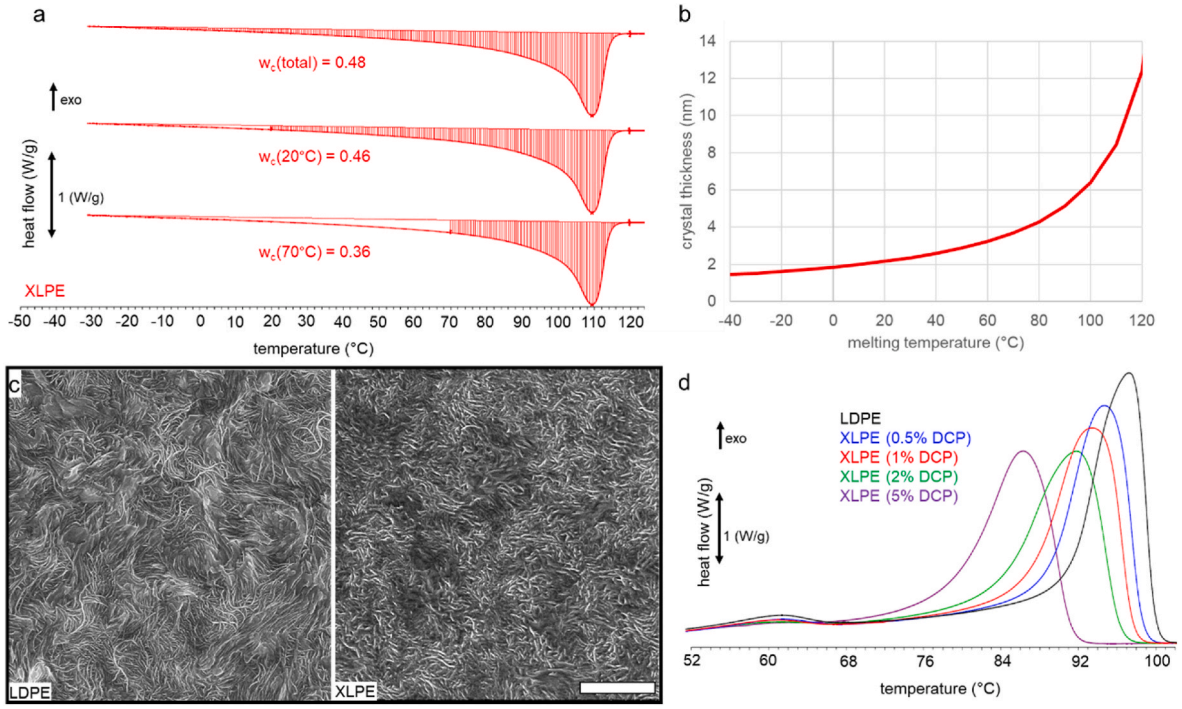


Fig. 5. Semicrystalline microstructure assessed by DSC; a) crystallinity at different temperatures from the second heating thermogram, b) crystal thickness distribution according to Thomson–Gibbs equation, c) crystal thickness distribution shown by SEM, the scale bar is 1 μm [33], d) crystallization thermogram. a, b, and d) these data are original and obtained for this publication, c) Reproduced with permission [33] Copyright 2016, IEEE.

hypothetically fractioned into small rectangles with a width of a small temperature range, which corresponds to specific crystal thickness according to the Thomson–Gibbs equation, Fig. 5b. The crystal thickness (L_c) is calculated according to the Thomson–Gibbs equation (eqn. (1)) depending on the melting temperature (T_m) [16]:

$$L_c = \frac{2\sigma_e}{\Delta H_f^o \rho_c \left(1 - \frac{T_m}{T_m^o}\right)} \quad \text{(eqn. 1)}$$

where T_m is the melting temperature, $\rho_c = 1003.0$ kg m^{-3} and $\rho_a = 851.9$ kg m^{-3} are the densities of the crystalline and amorphous components, respectively, and $\sigma_e = 93$ mJ m^{-2} is the fold surface free energy for linear polyethylene. The length of small rectangles in Fig. 5a indicates the amount of crystal with a specific thickness. Therefore, it is possible to obtain the crystal thickness distribution. Fig. 5c shows the SEM images of cryo-fractured surfaces of melt-processed LDPE and XLPE after acid etching (a harsh process to dissolve away the amorphous phase and reveal the semicrystalline morphology) [33]. For these images, the crystal thickness distribution is shown visually, which corresponds to the crystal thickness obtained from the DSC thermogram and Thomson–Gibbs equation.

The mass crystallinity (w_c) is determined according to the total enthalpy method, $w_c = \Delta H_f / \Delta H_f^\circ$, where ΔH_f is the measured melting enthalpy, ΔH_f° is the melting enthalpy for 100 % crystalline PE (293 J/g) at the equilibrium melting point of T_m° (141.5 °C). This is a simplified version for obtaining the crystallinity, however, for a more precise method, the heat capacities of amorphous and crystalline parts should be implemented in the enthalpy method [34]. It should be noted the method has some errors (ca. 5 %) based on selecting the baseline. The crystallinity at a given temperature ($w_c(T)$) within the melting temperature range was obtained by $\Delta H_f\ (T)$ by truncating the broad melting peak at this temperature. For example, in Fig. 5a the crystallinity at different temperatures is shown. Therefore, when characterizing PE it is important to state the crystallinity and the corresponding temperature together. The corresponding temperature could be either storage, operating, or post-treatment temperatures in cable production.

The intermediate cooling gives information about the crystallization temperature. Fig. 5d shows the DSC cooling of XLPE samples crosslinked with different content of DCP. It is shown that the crystallization temperature is reduced from 97 to 86 °C by increasing DCP content from 0 % to 5 %. In some literature, the onset of crystallization is indirectly related to the spherulite size meaning that a higher onset of crystallization temperature leads to smaller spherulites [16]. This is related to the nucleation effect, wherein an additive (e.g. nucleating agents, and nanoparticles) creates more nuclei during crystallization, which in turn increases the number of spherulites with smaller sizes. This cannot be applied to XLPE with different content of DCP, since the addition of DCP changes the shape of spherulites from spherulite to axialites, and crystal sizes reduce while the crystallization temperature and onset of crystallization decrease [31]. The presence of crosslinks is reported to increase nucleation, and the formation of extensive morphological features is therefore suppressed, as revealed by SEM images [33,35].

During cooling, another peak is detected in the range of 50–70 °C in the DSC thermogram, wherein the α relaxation occurs as well, see Fig. 5d. It is difficult to state that this DSC peak is either exactly α relaxation or a crystal thickening due to α relaxation (See Fig. 4c). It should be noted that this peak is not present in the heating thermograms. This process is thoroughly explained by Boyd [32], and is discussed briefly here. The presence of α relaxation could be detected in loss modulus (mechanical, measured by dynamic mechanical analysis (DMA)) or imaginary part of permittivity (dielectric, measured by dielectric spectroscopy). The mechanical and dielectric α relaxations are shown differently in molecular motion and microstructure. The dielectric one involves the twist of the crystal and could be triggered by switching the electric field, while the mechanical one involves relaxation in both crystalline and amorphous regions. This is primarily caused by longitudinal chain transport through the crystallites of the semicrystalline polymer, which in turn results in the reorganization of the adjacent amorphous and crystalline regions, See Fig. 4c. The α process needs low activation energy and leads to crystal thickening. This important feature occurs during the thermal cycling of XLPE insulation, which is seldom addressed in the literature.

In general, in this Section, the concept of semicrystalline morphology and microstructure was shown with the terms of crystallinity, crystal thickness, crystallization, and spherulite size using DSC. The presence of α relaxation process leads to crystal thickening. The extrusion, curing, cooling, and post-extrusion degassing processes alter the microstructure. In the next Section, two case studies will be shown to highlight the impact of the process on microstructure and consequently on macroscale DC conductivity.

4. The link between microstructure and DC conductivity

As stated earlier, several parameters could impact the level of DC conductivity and the appearance of DC conductivity peaks during thermal cycling. The presence of crosslinking byproducts and other types of impurities (e.g. migration of contamination from protective film to XLPE during hot-press) could increase the level of DC conductivity and the appearance of the peak [10,27,28]. After degassing of byproducts at elevated temperature and vacuum, the level of DC conductivity was reduced by almost one order of magnitude, and the conductivity peak disappeared during thermal cycling (the intensity of the peak became smaller after each thermal cycling) [9,10]. It should be noted that during degassing the volatile species would be removed, but not necessarily all contaminations. During the degassing of plaque samples, the XLPE experiences elevated temperatures (50–70 °C), which lead to the α relaxation process and crystal thickening. Therefore, during the degassing post-process two events occur in XLPE:

1. Removal of volatiles.
2. Molecular motion and morphology change (from the molecular level to the micro-scale).

In our previous study, a series of experiments were performed on different XLPE plaque samples to separate these two events [9]. Apart from non-degassed and degassed samples, an annealed sample was prepared, wherein the sample was encapsulated to avoid any volatile removal, and then placed in an oven with the same temperature as degassing temperature (not vacuum). In this way, the annealed sample had the same thermal history (see above-mentioned event 2) as the degassed sample, while the volatiles were kept. In this way, the volatile parameter was ruled out. These samples were analyzed with DC conductivity and DSC measurements to reveal the link between the microstructure and DC conductivity, Fig. 6. The overall characteristics of these samples are outlined in Table 1.

The non-degassed sample shows DC conductivity peak/knee during heating and cooling, as shown by arrows in Fig. 6a. The peaks became weaker after the first thermal cycle. The degassed sample shows lower conductivity than the non-degassed sample due to the removal of byproducts. There is no peak detected in the DC conductivity for the degassed sample. The annealed sample with kept byproducts did not show the DC conductivity peaks either, like the degassed sample, during cooling. From this observation, it could be suggested that the disappearance of the conductivity peak is related to the thermal history and microstructure of the sample.

Fig. 6b shows the first DSC heating thermograms to see the effect of thermal history. The degassed, annealed, and non-degassed samples (before DC conductivity measurement), and the non-degassed sample after DC conductivity show a shoulder peak in DSC thermograms. According to the Thomson–Gibbs equation, as shown in Fig. 5b, this additional peak shoulder corresponds to the crystal thickness of ca. 4

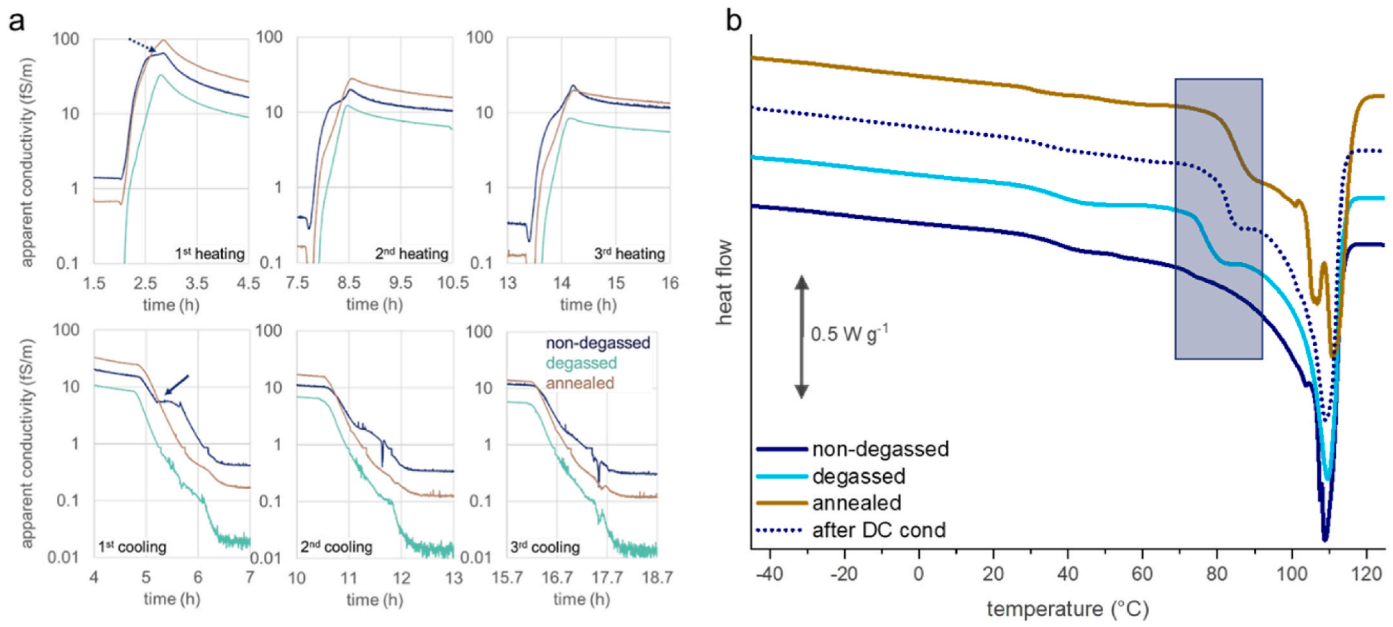


Fig. 6. The link between DC conductivity and microstructure of XLPE samples pressed with Al protection film, a) the DC conductivity during heatings and coolings between 20 and 70 °C (See the thermal cycle Fig. 3b bottom), b) the first DSC heating thermogram showing the thermal history (the "non-degassed", "degassed" and "annealed" samples are before DC conductivity measurement. The "after DC cond" is the non-degassed sample after DC conductivity measurement with at least three thermal cyclings). The highlighted square shows the appearance of the "annealing" DSC peak [9]. Copyright 2022, with permission from IEEE.

Table 1
Summary of the plaque XLPE samples.

XLPE designation	Post-treatment	Presence of volatile[a]	Microstructure change after crosslinking	Presence of DC peaks
Non-degassed	None	Yes	None	Yes
Degassed	Degassing at 70 °C under vacuum	No	Crystal thickening via α relaxation	No
Annealed	Annealing at 70 °C under atmospheric pressure (encapsulated)	Yes	Crystal thickening via α relaxation	No

[a] The presence of volatile was checked with thermogravimetric analysis (TGA) and gas chromatography-mass spectrometry (GC-MS) (not shown here).

nm. This means that the XLPE sample after exposure to the thermal history either by degassing, annealing, or thermal cycling in DC conductivity obtained more crystals with this thickness than the non-degassed XLPE sample. This is referred to as the "annealing" DSC peak (See highlighted square in Fig. 6b), which appears ca. 10–20 °C above the storage, usage, or annealing temperature in the DSC thermogram due to crystal "perfection" or "thickening". Here, the highest temperature for annealing, degassing, and DC conductivity measurements was 70 °C, which resulted in the appearance of a shoulder peak in the 1st heating DSC thermogram around 80 °C (it should be noted the shoulder peak intensity and temperature are related to the time and size of the sample during annealing). As stated earlier, the crystal thickening could occur after α relaxation and then lead to reorganization of the crystalline structure. However, here it is not clear whether α relaxation itself or the new semicrystalline structure could result in a DC conductivity peak. Ieda [36] showed that such relaxation processes could create deep/-shallow traps, and it is known that the presence of traps could alter the charge mobility and in consequence the DC conductivity. It was also suggested that the crystalline and amorphous parts of PE have different charge transport behavior [16]. The change in the semicrystalline structure during different polymer processing and post-processing could also result in different charge mobility or DC conductivity. Therefore, the α relaxation and crystal perfection due to thermal cycling, degassing, and annealing could both result in DC conductivity behavior change.

In another study [37], the link among process, microstructure, and DC conductivity was shown for LDPE. The extrusion of LDPE pellets for 10 s and 6 min results in 5 μm spherulites and random lamellae (without distinctive spherulites) superstructures, respectively, as revealed by SEM imaging. The size of spherulites could be indirectly determined by crystallization temperature using of DSC cooling thermogram, wherein the lower crystallization temperature corresponds to bigger spherulites (See nucleation concept in the Microstructure Section). The bigger spherulites because of the shorter extrusion process, result in larger DC conductivities. In another case for LDPE, it was shown that the larger spherulitic microstructure created by a shorter extrusion process led to larger DC conductivities [37].

Here, for an XLPE case it was shown that by ruling out of byproduct volatile parameter, the DC conductivity peak during thermal cycling disappeared in a post-heat-treatment process, i.e. annealing, due to crystal thickening [9]. Therefore, the link among process – microstructure – properties (DC conductivity) for XLPE and LDPE was shown.

5. Limitations

In this article, several methods based on different instruments were suggested, microscopy, DSC, DMA, dielectric spectroscopy, and DC conductivity. One important concern on all methods is the sample size and heat transfer, and whether this sample size can represent the whole cable insulation. For example, the DSC is a good method for microstructure study, where the sample size is around a few microliters, wherein the fast heat transfer is easily achievable for such a small sample. However, a cable insulation layer is ca. 20 mm thick, and the temperature inhomogeneity could be significantly high. Therefore, it is difficult to claim that the whole insulation has a similar microstructure resulting in a specific DC conductivity trend.

The apparent DC conductivity here is shown for plaque samples during short thermal cycling, however, the DC conductivity of real cable models could be longer and more cycling steps.

6. Conclusions

The link among microstructure, process, and a macro-scale property of DC conductivity was highlighted for the XLPE HVDC insulations. The link is important to further understand and improve the characteristics of insulation. The microstructure of the XLPE sample could be altered by thermal history during the main processing (extrusion, compression molding) and post-processing (cooling, degassing, annealing, thermal cycling). The underlying mechanism is related to the thermal relaxation processes that change the molecular/chain motion in both crystalline and amorphous phases. The relaxation ultimately results in the reorganization or perfection of the semicrystalline structure. These relaxations and perfections impact the DC conductivity (both level and disappearance of the peaks). This article shows that the insulating performance could be improved with the insight of link process – microstructure – macro-scale property in the bottom-up strategies.

7. Outlook

In this article, the use of conventional DSC was highlighted, however, the Temperature-Modulated DSC (TM-DSC) is a newer method that the sample is exposed to periodical modulation in the ramp of heating and cooling. In this way, thermodynamically reversible such as melting transition could be distinguished from non-reversing processes, such as recrystallization, crystal annealing, and perfection of non-equilibrium crystals [38].

In this article, the impact of nanometer- and micrometer-sized semicrystalline phases in XLPE on the macroscopic properties e.g. DC conductivity was shown. Recently, new techniques have been developed to directly observe the charge transport on the nanometric and micrometer scales to reveal macroscopic properties such as intermodulation electrostatic force microscopy (ImEFM) [16,39,40]. This new technique could map the charge transport in the nanometer scale in the semicrystalline structure of XLPE, and therefore the link between semicrystalline microstructure and macroscale property of DC conductivity and surface potential could be directly observed. Therefore, this article encourages the researchers to contribute such new nanoprobing techniques in finding the link of the process – microstructure – macro-scale property.

CRediT authorship contribution statement

Amir Masoud Pourrahimi: Writing – review & editing, Writing – original draft, Validation, Supervision, Investigation, Conceptualization. **Claire Pitois:** Writing – review & editing, Project administration, Investigation. **Amirhossein Abbasi:** Writing – review & editing, Validation, Project administration, Investigation.

Declaration of competing interest

The authors declare that they have no known competing financial interests or personal relationships that could have appeared to influence the work reported in this paper.

Data availability

Data will be made available on request.

Acknowledgments

Dedicated to Prof. Ulf W. Gedde on the occasion of his 71st birthday. Professor Ulf W. Gedde is acknowledged for valuable feedback.

References

[1] A. Felgel-Farnholz, A. Schweighuber, C.W. Klampfl, J. Fischer, Comparative study on the degradation of HDPE, LLDPE and LDPE during multiple extrusions, Polym. Degrad. Stabil. 216 (2023) 110486.
[2] L.W. McKeen, Permeability Properties of Plastics and Elastomers, Elsevier Science, 2016.
[3] X.M. Zhang, S. Elkoun, A. Ajji, M.A. Huneault, Oriented structure and anisotropy properties of polymer blown films: HDPE, LLDPE and LDPE, Polymer 45 (2004) 217–229.
[4] U.W. Gedde, M.S. Hedenqvist, Fundamental Polymer Science, Springer, 2019.
[5] A. Moyassari, H. Mostafavi, T. Gkourmpis, M.S. Hedenqvist, U.W. Gedde, F. Nilsson, Simulation of semi-crystalline polyethylene: effect of short-chain branching on tie chains and trapped entanglements, Polymer 72 (2015) 177–184.
[6] C.K. Georgantopoulos, M.K. Esfahani, I.F.C. Naue, M. Wilhelm, R. Kádár, Role of molecular architecture and temperature on extrusion melt flow instabilities of two industrial LLDPE and LDPE polyethylenes investigated by capillary rheology, high-pressure sensitivity slit die and optical analysis, J. Appl. Polym. Sci. 140 (2023) e53165.
[7] S. Kumara, A.M. Pourrahimi, A. Soroudi, X. Xu, T. Hammarström, Y. Serdyuk, C. Müller, Invariant electrical conductivity upon thermal ageing of a crosslinked copolymer blend for high voltage insulation, Mater. Adv. 3 (2022) 4718–4723.
[8] S. Kumara, X. Xu, T. Hammarström, Y. Ouyang, A.M. Pourrahimi, C. Müller, Y. V. Serdyuk, Electrical characterization of a new crosslinked copolymer blend for DC cable insulation, Energies 13 (2020) 1434.
[9] A.M. Pourrahimi, S.W. Cho, S. Anwar, M. Saleemi, C. Pitois, A. Abbasi, The Role of Thermal Relaxations and Semicrystalline Microstructure in Charging Currents of XLPE, 2022 IEEE 4th International Conference on Dielectrics (ICD), 2022, pp. 158–161.
[10] H. Ghorbani, Characterization of Conduction and Polarization Properties of HVDC Cable XLPE Insulation Materials, TRITA-EECS-AVL, KTH Royal Institute of Technology, stockholm, 2018.
[11] H. Orton, History of underground power cables, IEEE Electr. Insul. Mag. 29 (2013) 52–57.
[12] 640 kV Extruded HVDC Cable System, NKT HV Cables AB, 2017.
[13] A. Abbasi, M. Jeroense, Fully qualified low loss 525 and 640 kV extruded DC cable systems, Power Eng. J. 20 (2018) 4–10.
[14] M. Jeroense, P. Bergelin, T. Quist, A. Abbasi, H. Rapp, L. Wang, Fully Qualified 640 kV Underground Extruded DC Cable System, CIGRE Session, 2018. Paper B1-309.
[15] A.M. Pourrahimi, S. Kumara, F. Palmieri, L. Yu, A. Lund, T. Hammarström, P.-O. Hagstrand, I.G. Scheblykin, D. Fabiani, X. Xu, C. Müller, Repurposing poly(3-hexylthiophene) as a conductivity-reducing additive for polyethylene-based high-voltage insulation, Adv. Mater. 33 (2021) 2100714.
[16] A.M. Pourrahimi, R.T. Olsson, M.S. Hedenqvist, The role of interfaces in polyethylene/metal-oxide nanocomposites for ultrahigh-voltage insulating materials, Adv. Mater. 30 (2018) 1703624.
[17] A.M. Pourrahimi, L.K.H. Pallon, D. Liu, T.A. Hoang, S. Gubanski, M.S. Hedenqvist, R.T. Olsson, U.W. Gedde, Polyethylene nanocomposites for the next generation of ultralow-transmission-loss HVDC cables: insulation containing moisture-resistant MgO nanoparticles, ACS Appl. Mater. Interfaces 8 (2016) 14824–14835.
[18] M. Mauri, Alternative Polyethylene Crosslinking Concepts for Power Cable Insulation, Chalmers Tekniska Hogskola (Sweden), Gothenburg, Sweden, 2019.
[19] M. Ahmed, L. Zhong, F. Li, N. Xu, J. Gao, Improving the DC dielectric properties of XLPE with appropriate content of dicumyl peroxide for HVDC cables insulation, Materials 15 (2022) 5857.
[20] S. D'Auria, A.M. Pourrahimi, A. Favero, P. Neuteboom, X. Xu, S. Haraguchi, M. Bek, R. Kádár, E. Dalcanale, R. Pinalli, C. Müller, J. Vachon, Polyethylene based ionomers as high voltage insulation materials, Adv. Funct. Mater. 33 (2023) 2301878.
[21] Y. Ouyang, A.M. Pourrahimi, I. Östergren, M. Mellqvist, J. Ånevall, A. Soroudi, A. Lund, X. Xu, T. Gkourmpis, P.-O. Hagstrand, C. Müller, Highly insulating thermoplastic blends comprising a styrenic copolymer for direct-current power cable insulation, High Volt. 7 (2022) 251–259.
[22] A. Harlin, P. Huotari, Quality aspects on the power cable core insulation extrusion and thermal curing process, Int. Polym. Process. 18 (2003) 291–297.
[23] D. Liu, A.M. Pourrahimi, L.K.H. Pallon, C.C. Sánchez, R.T. Olsson, M.S. Hedenqvist, L. Fogelström, E. Malmström, U.W. Gedde, Interactions between a phenolic antioxidant, moisture, peroxide and crosslinking by-products with metal oxide nanoparticles in branched polyethylene, Polym. Degrad. Stabil. 125 (2016) 21–32.
[24] A. Smedberg, J. Böstrom, P. Houotari, M. Bengtsson, The degassing process of HV XLPE cables and its influence on selected electrical properties. Proceedings of the 9th International Conference on Insulated Power Cables, Versailles, France, 2015, pp. 21–25.
[25] F.-B. Meng, X. Chen, X. Xu, C. Dai, A. Paramane, Y. Tanaka, Effect of degassing treatment durations on physico-chemical and electrical properties of 500 kV extra HVDC XLPE cable insulation, Polym. Degrad. Stabil. 188 (2021) 109566.
[26] T. Andrews, R.N. Hampton, A. Smedberg, D. Wald, V. Waschk, W. Weissenberg, The role of degassing in XLPE power cable manufacture, IEEE Electr. Insul. Mag. 22 (2006) 5–16.
[27] H. Ghorbani, M. Saltzer, C.O. Olsson, Observation of Non-monotonic Dependence of Leakage Current with Temperature during Thermal Cycling, 2016 IEEE Electrical Insulation Conference, EIC), 2016, pp. 488–491.
[28] H. Ghorbani, C.O. Olsson, A. Abbasi, M. Saltzer, Influence of Press Films on Conduction in Polyethylene Plaque Samples, 2016 IEEE International Conference on Dielectrics (ICD), 2016, pp. 1179–1182.

[29] A. Abbasi, M. Jeroense, Conductivity and Space Charge Dynamics of XLPE Samples during Temperature Cycling, 2018 IEEE 2nd International Conference on Dielectrics (ICD), 2018, pp. 1–4.
[30] M. Mauri, A.I. Hofmann, D. Gómez-Heincke, S. Kumara, A.M. Pourrahimi, Y. Ouyang, P.-O. Hagstrand, T. Gkourmpis, X. Xu, O. Prieto, C. Müller, Click chemistry-type crosslinking of a low-conductivity polyethylene copolymer ternary blend for power cable insulation, Polym. Int. 69 (2020) 404–412.
[31] S. Nilsson, T. Hjertberg, A. Smedberg, Structural effects on thermal properties and morphology in XLPE, Eur. Polym. J. 46 (2010) 1759–1769.
[32] R.H. Boyd, Relaxation processes in crystalline polymers: molecular interpretation — a review, Polymer 26 (1985) 1123–1133.
[33] F. Abid, H. Ghorbani, A.M. Pourrahimi, H. Edin, Differences in morphology and polarization properties of heat-treated XLPE and LDPE insulation, in: 2016 IEEE Conference on Electrical Insulation and Dielectric Phenomena, CEIDP), 2016, pp. 113–116.
[34] A.P. Gray, Polymer crystallinity determinations by DSC, Thermochim. Acta 1 (1970) 563–579.
[35] T. Andritsch, A. Vaughan, G.C. Stevens, Novel insulation materials for high voltage cable systems, IEEE Electr. Insul. Mag. 33 (2017) 27–33.
[36] M. Ieda, Electrical conduction and carrier traps in polymeric materials, IEEE Trans. Electr. Insul., EI- 19 (1984) 162–178.
[37] M.E. Karlsson, X. Xu, H. Hillborg, V. Ström, M.S. Hedenqvist, F. Nilsson, R. T. Olsson, Lamellae-controlled electrical properties of polyethylene – morphology, oxidation and effects of antioxidant on the DC conductivity, RSC Adv. 10 (2020) 4698–4709.
[38] A. Scoppio, D. Cavallo, A.J. Müller, D. Tranchida, Temperature modulated DSC for composition analysis of recycled polyolefin blends, Polym. Test. 113 (2022) 107656.
[39] R. Borgani, L.K.H. Pallon, M.S. Hedenqvist, U.W. Gedde, D.B. Haviland, Local charge injection and extraction on surface-modified Al2O3 nanoparticles in LDPE, Nano Lett. 16 (2016) 5934–5937.
[40] R. Borgani, D. Forchheimer, J. Bergqvist, P.-A. Thorén, O. Inganäs, D.B. Haviland, Intermodulation electrostatic force microscopy for imaging surface photo-voltage, Appl. Phys. Lett. 105 (2014).